Final Draft
of the original manuscript:

Plaine, A.H.; Gonzalez, A.R.; Suhuddin, U.F.H.; dos Santos, J.F.;
Alcantara, N.G.:

**The optimization of friction spot welding process parameters in
AA6181-T4 and Ti6Al4V dissimilar joints**

The optimization of friction spot welding process parameters in AA6181-T4 and Ti6Al4V dissimilar joints

A. H. Plaine[a,b*], A. R. Gonzalez[c], U.F.H. Suhuddin[a], J. F. dos Santos[a], N. G. Alcântara[b]

Affiliation

[a] Helmholtz-Zentrum Geesthacht, Institute of Materials Research, Materials Mechanics, Solid-State Joining Processes, Max-Planck-Str. 1, Geesthacht, Germany.
[b] Federal University of São Carlos, Materials Engineering Department, R. Washington Luís Km 235 - SP 310, Sao Carlos, Brazil.
[c] Federal University of Rio Grande do Sul, Mechanical Engineering Department, Av. Paulo Gama, 110 Farroupilha, Porto Alegre, Brazil
* Corresponding author: athosplaine@hotmail.com

Abstract

Friction spot welding is a relatively new solid-state joining process able to produce overlap joints between similar and dissimilar materials. In this study, the effect of the process parameters on the lap shear strength of AA6181-T4/Ti6Al4V single joints was investigated using full-factorial design of experiment and analyses of variance. Sound joints with lap shear strength from 4769 N to 6449 N were achieved and the influence of the main process parameters on joint performance was evaluated. Tool rotational speed was the parameter with the largest influence on the joint shear resistance, followed by its interaction with dwell time. Based on the experimental results following response surface methodology, a mathematical model to predict lap shear strength was developed using a second order polynomial function. The initial prediction results indicated that the established model could adequately estimate joint strength within the range of welding parameters being used. The model was then used to optimize welding parameters in order satisfy engineering demands.

Keywords

Friction spot welding; Aluminum alloy; Titanium alloy; Dissimilar joint; Design of experiments; Response of surface methodology.

Highlights

- Friction spot welding of AA6181-T4/Ti6Al4V single-lap joints was demonstrated.

- The influence of joining parameters on joint mechanical performance was determined

- A mathematical model for estimating lap shear strength was successfully established.
- A set of welding parameters was obtained to produce economic and efficient joints.

1. Introduction

It is known that advanced dissimilar lightweight structures consisting of multi material become more and more attractive, especially in the transportation sector [1-4]. This has been supported by the need to offer a distinct combination of properties required to manufacture lighter, safer, more environmentally friendly and ultimately cheaper structures. Aluminum alloys are desirable in these fields due to its low density and cost. Titanium alloys are also promising materials because of their high specific strength and corrosion resistance [5-7]. However, joining of aluminum and titanium alloys still a complex task due to their large differences in physical and chemical properties. The available techniques are either too expensive, limited in performance or are not environmental friendly [1,8]. Consequently, the practical success of joining such materials depends on the development of new joining technologies.

Friction spot welding (FSpW), also known as refill friction stir spot welding, is a relative new solid-state joining process which stands up as an alternative for producing dissimilar overlap spot joints. The process uses a non-consumable tool consisting of two movable parts – pin and sleeve – mounted coaxially to a clamping ring, as presented in Fig.1. A schematic illustration of the FSpW process is shown in Fig. 2. In the first stage, the upper and lower plates are fixed together by the clamping ring and the backing anvil, meanwhile both the pin and the sleeve start to rotate. In the second stage, pin and sleeve move in opposite direction to each other; one is plunged into the material while the other moves upwards, creating a space (reservoir) where the plasticized material is accommodated. Rotating pin and sleeve generates frictional heating, plasticizing a volume of material underneath the tool. In the third stage, after reaching the pre-set plunge depth and dwell time, pin and sleeve retract back to the surface of the plate forcing the displaced material to completely refill the keyhole. In the last stage, the tool is removed from the plate surface, and a weld without keyhole is left.

Fig. 1. Friction spot welding tool.
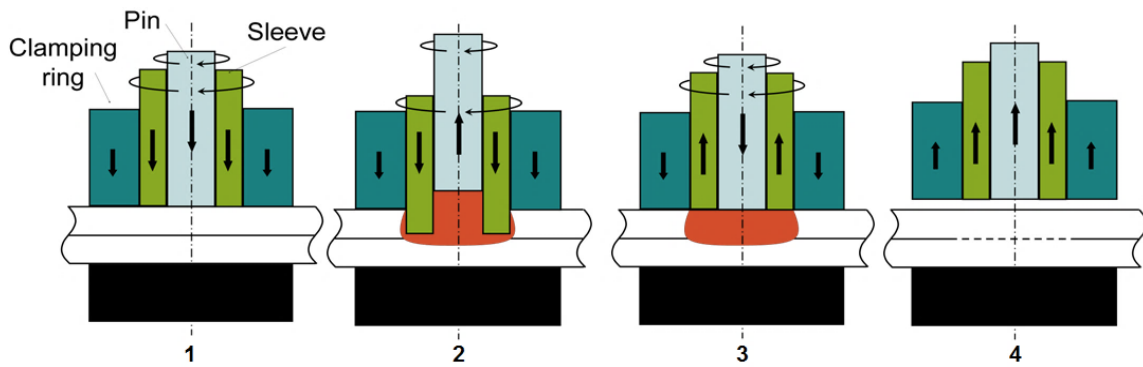
Fig. 2. Illustration of FSpW process using sleeve plunge variant: 1) Clamping and tool rotation; 2) Sleeve plunge and the pin retraction; 3) Parts back to surface level; and 4) Tool removal.

The main benefits of using FSpW for joining aluminum and titanium alloys are related to its low temperature cycles, which can minimize the formation of the undesirable Ti–Al intermetallic compounds [9], and geometry compatibility to replace rivets, the most widely used technique to join dissimilar materials in the automotive and aircraft industries [10]. Moreover, solid state processes generally consumes less energy in comparison to other fusion welding processes, like resistance spot welding (RSW), especially for aluminum alloys [11]. Previous works of FSpW on dissimilar joints such as AA6181 and AZ31, AA6181-T6 and DP600 (with and without galvanized layer) and AA5457-H22 and DP600 (with and without galvanized layer) have shown promising results [12]. These joints showed similar or superior mechanical performance compared to other dissimilar joints produced with state-of-the-art techniques.

The Full-Factorial Design (FFD) is a powerful statistical method that enables optimizing the performance of a product, process, design and system with a significant reduction in time and costs. When combined with the use of analysis of variance (ANOVA) and Response Surface Methodology (RSM), FFD can be used to determine the relative importance of the welding process parameters on joint properties and to efficiently obtain the optimal process response. The FFD is most adequate in situations where a reduced number of factors and levels are selected. In FSpW this scenario can be achieved by properly choosing the main process parameters and their ranges based on initial trials.

Amancio-Filho et al. [13] investigated the influence of FSpW process parameters on the strength of overlap welds on AA2024-T3 alloy produced using a 3^2 FFD. They showed that dwell time (DT) has the main effect on the weld strength, followed by rotational speed (RS) and DT interaction. Altmeyer et al. [14] successfully used a 2^4 FFD to explain the effect of the friction riveting process parameters on the joint formation and performance of Ti alloy/short-fibre reinforced polyether ether ketone joints. Dashatan et al. [15] conducted experimental tests according to a 3^3 FFD for friction stir spot welding of dissimilar polymethyl methacrylate and acrylonitrile butadiene styrene sheets to optimize the shear strength. Their results pointed out that all the three process parameters analyzed had a significant effect on the response. Olabi et al. [16] used a 3^3 FFD and Taguchi designs combined with RSM to effectively minimize the residual stresses in laser welded structures.

In this work, the 3^k FFD method and ANOVA were used to investigate the influence of RS and DT on the lap shear strength (LSS) of AA6181-T4 and Ti6Al4V dissimilar joints produced by FSpW. The RSM was also applied to predict the LSS with respect to the tested process parameters. The established model was also used to optimize the process parameters considered to produce joints with less energy consumption and high efficiency.

2. Experimental procedure

Rolled aluminum alloy AA6181-T4 and titanium alloy Ti6Al4V plates with the dimensions of 100×25.4×1.5 mm were used in this work. Table 1 lists the nominal chemical composition of the two alloys. Prior to joining, the parts were slightly ground with P1200 SiC sandpaper to remove inhomogeneous natural oxide layer and cleaned with acetone to remove surface contaminations.

Table 1. Nominal chemical compositions and of base materials (wt.%).

Alloys	Ti	Al	Si	Fe	Cu	Mn	Mg	Cr	Zn	V	C	O	N	H
AA6181-T4	0.023	Bal.	0.85	0.25	0.06	0.09	0.74	0.013	0.012	-	-	-	-	-
Ti6Al4V	Bal.	6.25	-	0.14	-	-	-	-	-	3.91	0.023	0.126	0.003	0.002

Overlap single joints were performed using a RPS 200 friction spot welding machine and a non-consumable tool with diameters of 18 mm, 9 mm and 6.4 mm for the clamping ring, sleeve and pin, respectively. The aluminum alloy sheet was placed over the titanium alloy sheet with the tool sleeve plunge remaining in the top sheet to avoid both excessive tool wear and excessive formation of intermetallic compounds. The mechanical performance of the joints was evaluated by means of LSS. Lap shear testing was performed using a universal testing machine Zwick–Roell model 1478 with crosshead speed of 2 mm/min at room temperature and specimen geometry in accordance with DIN EN ISO 14273 standard [17]. Three replicates were tested for each condition, and the LSS was calculated as the arithmetic mean of the replicates.

Table 2. FSpW process parameters and levels.

Symbol	Welding parameter	Unit	Level 1	Level 2	Level 3
RS	Rotational Speed	rpm	2000	2500	3000
DT	Dwell Time	s	1	3	5

A three-level FFD (3^k) with two factors (RS and DT) was selected for the evaluation of the LSS of the weld. Table 2 summarizes process parameters and levels used in this work. The range of welding parameters (levels), as the input for FFD experiments, was selected by preliminary visual analysis and performance. From these first observations, sleeve plunge depth and clamping ring force were kept constant in 1.4 mm and 12 kN, respectively. An ANOVA of the results obtained from FFD was performed to assess the influence of each FSpW process parameters and their interactions on the mechanical performance. In order to develop an adequate local functional relationship between the LSS and the FSpW process inputs, the RSM using a second-degree model was then applied. This model can be expressed mathematically as

presented in Eq. 1. From the model, a set of process parameters was determined with the aim of satisfying engineering demands for FSpW dissimilar joints of aluminum and titanium alloys.

$$y = \beta_0 + \sum_{i=1}^{k} \beta_i x_i + \sum \sum_{i<j} \beta_{ij} x_i x_j + \sum_{i=1}^{k} \beta_{ii} x_i^2 + \epsilon \tag{1}$$

3. Results and Discussions

Fig. 3 shows the appearance and the typical cross-section of a representative test specimen after joining. No defects or obvious reductions of thickness were observed in the weld. A higher-magnification micrograph acquired from the center of the joint (Fig. 3c) reveals the presence of a continuous layer of approximately 0.8 µm in thickness. The inset of Fig. 3c shows the corresponding EDS concentration profiles across diffusion zones, and it was found that a thin layer of $TiAl_3$ the solid solution of Si was formed in the interface. The identification and formation of phase components at the joint interface will be described in detail in another article. Although the exposure time of the interface was relatively short, nonetheless this time was apparently sufficient to induce the interdiffusion of Al and Ti atoms at the interface.

(a)

(b)

(c)
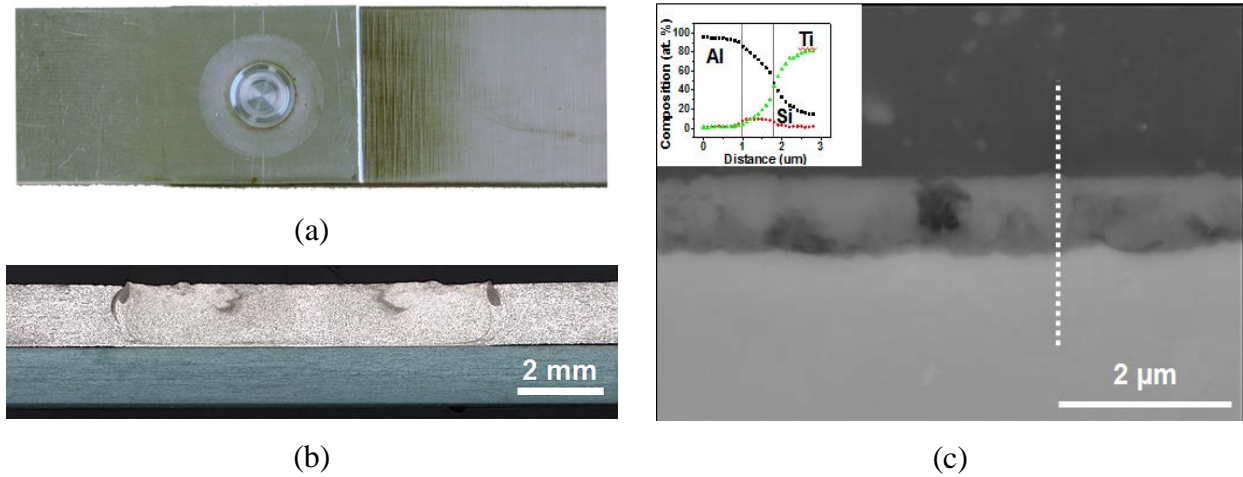
Fig 3. A representative image of the top view (a) and mid cross-section micrograph (b) of the joints. (c) Back-scattered electrons image of cross section, captured at the center of the joint, with the inset of the energy-dispersive X-ray spectroscopy concentration profile along the white line of the image.

According to the literature [18], the joining of aluminum and titanium alloys by traditional fusion welding methods is difficult because of the formation of excessive intermetallic compounds at the interface. Minimizing or optimizing Ti-Al intermetallic phases has become the key issue to achieve a robust Ti/Al dissimilar joint.

3.1. DOE: Three-level full-factorial (3^k FFD)

The FFD contains two factors on three levels, making the number of configurations N = $3^2 = 9$. The DOE test matrix along with the experimental values of LSS is shown in Table 3. The joints exhibited LSS varying from 4769 ± 73 N (condition 9) to 6449 ± 554 N (condition 5). The LSS average of all welds exceed the minimum required value of 3400N, according to AWS D17.2/D17.2M [19], for a 1.6 mm nominal thickness of Al alloys (the weakest material in the joint) having ultimate tensile strength from 240 to 386 MPa. Likewise, the maximum failure load reached (condition 5) was similar to the failure load of the optimized similar FSpW joint of AA6181-T4 reported by Rosendo et al. [20]. These outstanding results are probably associated with the reduction of the brittle intermetallic compounds formation in the interface by using FSpW. Tanaka et al. [21] established that joint strength increased exponentially with a decrease of IMC thickness for dissimilar friction stir welds of mild steel to aluminum alloys. Wu et al. [22] confirmed this trend by showing that high strength friction stir welds of AA6061 and Ti6Al4V were achieved due to the formation of a thin IMC layer at the joint interface.

Table 3. Summary of the 3^k-full factorial design conditions and the experimental values of LSS.

Condition	RS (rpm)	DT (s)	LSS (N)			Average LSS (N)
			1	2	3	
1	2000	1	5434	5160	5061	5218 ± 193
2	2000	3	4896	5325	5326	5182 ± 248
3	2000	5	5831	5209	5506	5515 ± 311
4	2500	1	5516	5737	5827	5693 ± 160
5	2500	3	6121	7089	6138	6449 ± 554
6	2500	5	5821	5596	5863	5760 ± 144
7	3000	1	5813	5399	5611	5608 ± 207
8	3000	3	4873	4681	5175	4910 ± 249
9	3000	5	4830	4789	4688	4769 ± 73

3.1.1 Analysis of variance (ANOVA)

An understanding of the influence of the welding parameters on weld performance is needed to accurately assess the optimal combinations of the parameter levels. This can be achieved by using the ANOVA. In performing the ANOVA, the mean of squared deviations due to each design parameter needs to be calculated. The mean of squared deviations is equal to the sum of squared deviations divided by the number of degrees of freedom associated with the design parameter. Then, the F value for each design parameter is simply calculated as the ratio of the mean of squared deviations to the mean of squared error. Usually, when $F > 4$, it means that the change of the design parameter has a significant effect on the quality characteristic.

Table 4 shows the ANOVA performed with the acquired data, for an interval of confidence of 95%. The results reveal that the RS and the interaction RS*DT are significant factors affecting the joints performance. For a better understanding, the F-value was rewritten in terms of the percentage of contribution of each factor on the total variation, thus indicating the degree of influence on the tested result. The factors are physically significant when its percentage of contribution is smaller than the error associated. Among the parameters, RS showed to be the most affecting parameter on the LSS of the joints (49.6%), followed by the interaction RS*DT (30.7%). However, DT itself seems to have no significant influence on the response LSS for the selected range of welding parameters. The total contribution rate of the FSW parameters was 82.4%.

Table 4. ANOVA of LSS values.

Source	SS	df	MS	F-value	Contrib. [%]
RS (rpm)	3729508	2	1864754	25.47	49.66
DT (s)	157706	2	78853	1.08	2.10
RS (rpm) DT (s)	2304202	4	576050	7.87	30.68
Error	1318005	18	73222		17.56
Total SS	7509421	26			

Fig. 4 shows the main effects plot for mean LSS. The dashed line shows the value of the total mean of LSS. The small contribution of the DT on LSS is represented by the flatter curve profile (Fig. 4a). In contrast, the importance of RS to the LSS is once again confirmed by a substantial variation in LSS (Fig. 4b). The joints resistance considerably increases with the increase of the RS from low to intermediate values. However, high RS values seem to be

prejudicial to the LSS of the joints, probably due to the formation of a significant amount of detrimental phases in the interface. Although the effect of the DT on the joint performance is not remarkable, its trend is similar to RS.

Two-dimensional plots of cell means or treatment combination means can provide insights into the presence of interactions between the two factors. Fig. 5 presents a two-dimensional plot between RS and DT in terms of the mean LSS. The different behavior of the curves confirms a remarkable interaction between the welding parameters and it may be associated with the changes in the heat input regime related to variations in the temperature cycles, thus affecting the diffusion process taking place at the interface. It can be better understood in terms of the flux of diffusing atoms, J, used to quantify the mass of atoms diffusing through unit area per unit time [23]. Suhuddin et al. [24] reported that the mechanical property that relates to LSS is affected by the thickness of the intermetallic compound and the morphology of the interfacial area. Therefore, it is reasonable to assume that a sound interface depends on the diffusion of an optimum number of atoms through the interface (J x time) to sufficiently consolidate the joint and form no excessive intermetallic compounds. According to Fick's law, J is directly proportional to temperature [23]. Since RS and DT are welding parameters that mainly affect temperature and time, respectively, joints with high resistance can be achieved by a proper balance of these two variables. Fig. 5 indicates that the joints with the highest strength were obtained when working with intermediate RS and DT, low RS and high DT or high RS and low DT, corroborating with the assumptions made.

(a)   (b)
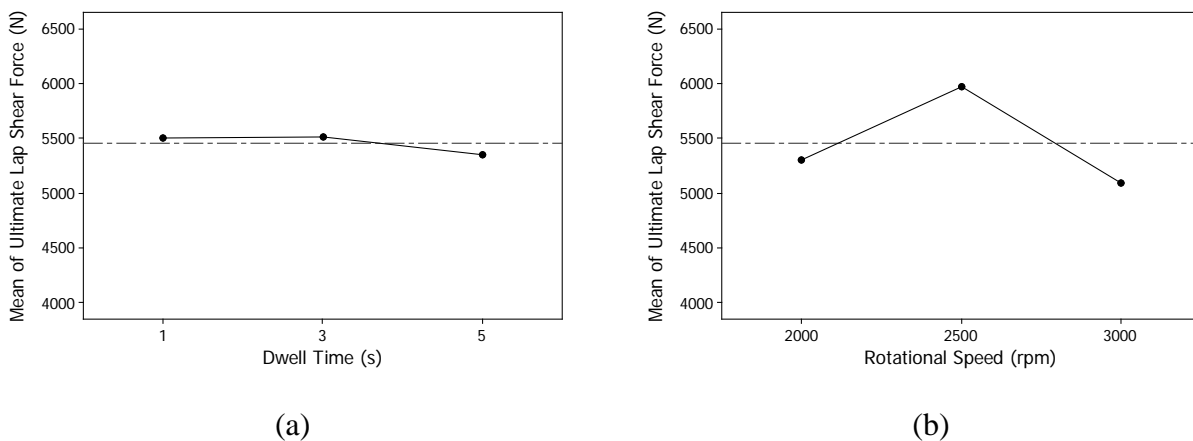
Fig. 4. Main effect plots of dwell time (a) and rotational speed (b) on the mean lap shear strength. The horizontal dashed line is referred to the average value of all observations in all

factor levels in the experiment (avg. LSS = 5456 N). The points in (a) and (b) are the means of LSS at the various levels of each factor (calculated from Table 3).
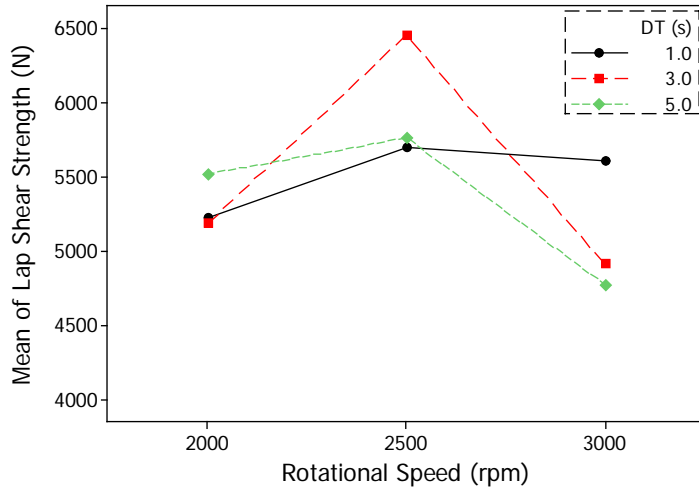
Fig. 5. Effects of the interaction between rotational speed and dwell time on the mean lap shear strength.

3.2. Response Surface Methodology (RSM)

Generally, the structure of the numerical relationship between the response and the independent variables is unknown. The first step in RSM is to find a suitable approximation to the true relationship. The most common forms are first or second-order polynomials. A second-order model can significantly improve the optimization process when a first-order model suffers lack of fit due to interaction between variables and surface curvature. Based on the results obtained from the FFD, a second-order regression model for LSS was developed in terms of the actual values of the significant factors, see Eq. 2. Note that each main effect was represented by a linear and a quadratic component, each with a single degree of freedom. Although the effect of a primary factor is not statistically significant, like DT, it must be considered in the numerical model if its interaction with others factors are significant.

$$LSS = 27717.29 - 19.146 * RS + 0.00399 * RS^2 - 35730.17 * DT + 5724.54 * DT^2$$
$$+ 29.8898 * RS * DT - 4.7477 * RS * DT^2 - 0.0061 * RS^2 * DT + 0.00095$$
$$* RS^2 * DT^2 \tag{2}$$

Eq. 2 is depicted in Fig. 6. It is clear that lower LSS occurs for extreme levels of RS and/or DT, whereas intermediate levels of both factors present higher values. This is due to the

importance of a proper balance of both time and temperature in the diffusion process for the interface formation. It can be also noted that the region where high values of resistance (> 6000N) can be achieved is considerable large, providing a wide process window for industrial applications.
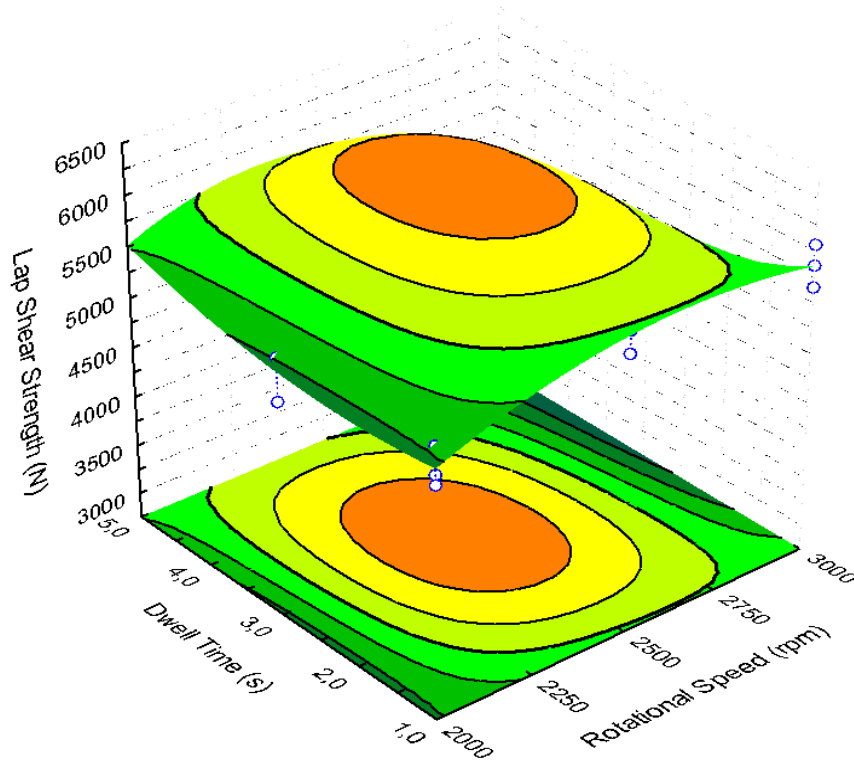
Fig. 6. Response surface plot for LSS as a function of RS and DT.

3.2.1. Verification of the developed model

The plot of the predicted versus actual values, shown in Fig. 7, indicates the satisfactory agreement between the response surface model and the actual values. The plot of the predicted versus actual values, shown in Fig. 7, indicates the satisfactory agreement between the response surface model and the actual values. In order to verify the adequacy of the developed model, three confirmation experiments were carried out with new process parameters chosen within the ranges from which the equation was derived. Table 5 shows the new process parameters in verifications 1, 2 and 3, where the actual and predicted values and the percentages of error are also included. Compared with the experimental data, the error of LSS prediction varies from 1.8% to 6.1%. The results indicate that the developed model has acceptable accuracy for LSS prediction.
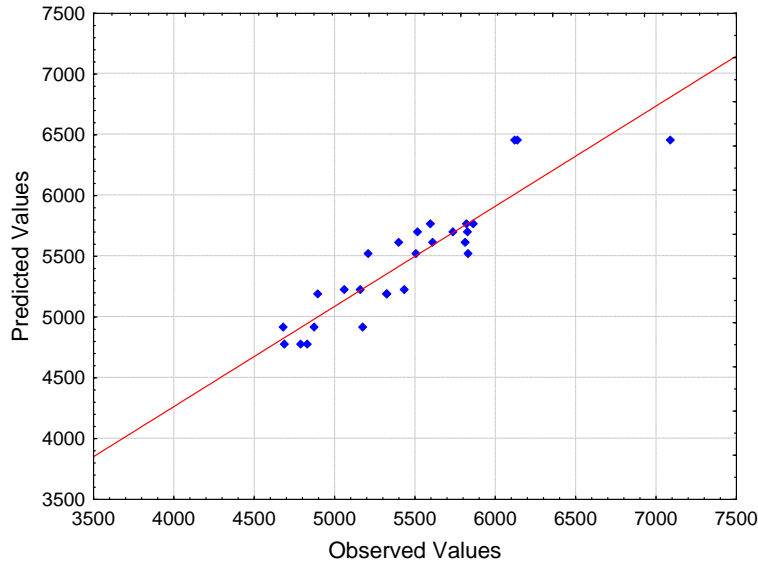
Fig. 7. Comparison of predicted LSS with experimental data.

Table 5. Experiment tests for model verification.

Verifications	Actual LSS (N)	Predicted LSS (N)	Error %
1 (RS = 2400 rpm, DT = 1.5 s)	5619	5983	6.1%
2 (RS = 2500 rpm, DT = 4.0 s)	6189	6302	1.8%
3 (RS = 3000 rpm, DT = 2.0 s)	4986	5212	4.3%

3.2.2. Optimization

In the numerical optimization a criteria was implemented in order to produce high performance joints with less energy consumption and high efficiency. As presented in Table 6, there are constrains on RS (minimum) and DT (minimum). The level of importance of each factor in terms of industrial application is represented by the "+" sign, varying from 1 to 5. Table 7 shows optimization analysis results based on their desirability (conversion of the response values into a dimensionless measure of performance, based on the weight or importance of the factors). The parameters of RS = 2500 rpm and DT = 2 s were chosen as the optimal operating parameters, by using a sleeve plunge depth of 1.4 mm and a clamping ring pressure of 12 kN.

Table 6. Optimization criteria and importance.

Variables	Criteria	Lower Limit	Upper Limit	Importance

RS (rpm)	Minimum	2000	2600	++
DT (s)	Minimum	1	3	++++
LSS (N)	Maximum	6000	-	+++++

Table 7. Optimal solutions based on the criteria.

N°	RS (rpm)	DT (s)	LSS (N)	Desirability
1	2300	2	6084	0.684
2	2400	2	6220	0.694
3	2500	2	6268	0.697
4	2600	2	6230	0.693
5	2200	3	6038	0.614
6	2300	3	6293	0.633
7	2400	3	6435	0.643
8	2500	3	6465	0.645
9	2600	3	6383	0.638

4. Conclusions

The effects of the friction spot welding process parameters on the mechanical strength of AA6181-T4 and Ti6Al4V dissimilar joints were investigated using statistical analysis. The following conclusions can be drawn based on the experimental and analytic results.

- The 3^2 full factorial designed experiments were successfully conducted. Produced joints showed good mechanical performance with lap shear strength varying from 4769 ± 73 N to 6449 ± 554 N.

- For the selected range of welding parameters, RS was the parameter with the largest influence on the lap shear strength of the joints (49.6%), followed by the interaction of RSxDT (30.7%). In contrast, DT showed to have no significant influence on the joints performance.

- A mathematical model for lap shear strength prediction was developed on the basis of RSM by utilizing the experimental results. The results indicated a satisfactory agreement between the predicted and the experimental values.

- Optimal, economic and efficient welds were achieved using the welding parameters (RS = 2500 rpm, DT = 2 s) obtained from the numerical optimization, for a sleeve plunge depth of 1.4 mm and a clamping ring pressure of 12 kN.

References

[1] Y. Wei, J. Li, J. Xiong, F. Huang, F. Zhang, S.H. Raza. Joining aluminum to titanium alloy by friction stir lap welding with cutting pin. Materials Characterization, 71 (2012), pp. 1-5.

[2] B. Majumdar, R. Galun, A. Weisheit, B.L. Mordike. Formation of a crack-free joint between Ti alloy and Al alloy by using a high-power CO_2 laser. Journal of Materials Science, 32 (1997), pp. 6191-6200.

[3] M.K. Lee, J.G. Lee, Y.H. Choi, D.W. Kim, C.K. Rhee, Y.B. Lee, S.J. Hong. Interlayer engineering for dissimilar bonding of titanium to stainless steel. Materials Letters, 64 (2010), pp. 1105–1108.

[4] M.S. Kenevisi, S.M. Mousavi Khoie. An investigation on microstructure and mechanical properties of Al7075 to Ti–6Al–4V Transient Liquid Phase (TLP) bonded joint. Materials & Design, 38 (2012), pp. 19–25.

[5] W.V. Vaidya, M. Horstmann, V. Ventzke, B. Petrovski, M. Koçak, R. Kocik, G. Tempus. Improving interfacial properties of a laser beam welded dissimilar joint of aluminium AA6056 and titanium Ti6Al4V for aeronautical applications. Journal of Materials Science, 45 (2010), pp. 6242-6254.

[6] Ren Jiangwei, Li Yajiang, Feng Tao. Microstructure characteristics in the interface zone of Ti/Al diffusion bonding. Materials Letters, 56 (2002), pp. 647–52.

[7] Jian Zhang, Yuan Xiao, Guoqiang Luo, Qiang Shen, Lianmeng Zhang. Effect of Ni interlayer on strength and microstructure of diffusion-bonded Mo/Cu joints. Materials Letters, 66 (2012), pp. 113-116.

[8] K. Bang, K. Lee, H. Bang, H. Bang. Interfacial Microstructure and Mechanical Properties of Dissimilar Friction Stir Welds between 6061-T6 Aluminum and Ti-6%Al-4%V Alloys. Materials Transactions, 52 (2011), pp. 974-978

[9] Y. Mishin, C. Herzig. Diffusion in the Ti–Al system. Acta Materialia, 48 (2000), pp. 589-623.

[10] M. Kreimeyer, F. Wagner, F. Vollertsen. Laser processing of aluminum–titanium-tailored blanks. Optics and Lasers in Engineering, 43 (2005), pp. 1021-1035.

[11] M. K. Kulekci, U. Esme, O. Er. Experimental comparison of resistance spot welding and friction-stir spot welding processes for the EN AW 5005 aluminum alloy. Materiali in Tehnologije 45 (2011), pp. 395-399.

[12] U. Suhuddin, L. Campanelli, M. Bissolatti, H. Wang, R. Verastegui, J.F. dos Santos. A review on microstructural and mechanical properties of friction spot welds in Al-based similar and dissimilar joints. Proceedings of the 1st International Joint Symposium on Joining and Welding (2013), pp. 15-21.

[13] S.T. Amancio-Filho, A.P.C. Camillo, L. Bergmann, J.F. dos Santos, S.E. Kuri, N.G. Alcântara. Preliminary Investigation of the Microstructure and Mechanical Behaviour of 2024 Aluminium Alloy Friction Spot Welds, Materials Transactions, 52 (2011), pp. 985-991.

[14] J. Altmeyer, J.F. dos Santos, S.T. Amancio-Filho. Effect of the friction riveting process parameters on the joint formation and performance of Ti alloy/short-fibre reinforced polyether ether ketone joints. Materials & Design, 60 (2014), pp. 164-176.

[15] S.H. Dashatan, T. Azdast, S.R. Ahmadi, A. Bagheri. Friction stir spot welding of dissimilar polymethyl methacrylate and acrylonitrile butadiene styrene sheets. Materials & Design, 45 (2013), pp. 135-141.

[16] A.G. Olabi, G. Casalino, K.Y. Benyounis, A. Rotondo. Minimisation of the residual stress in the heat affected zone by means of numerical methods. Materials & Design, 28 (2007), pp. 2295-2302.

[17] DIN EN ISO 14273. Specimen dimensions and procedure for tensile shear testing resistance spot, seam and embossed projection welds. In: DIN, the German Institute for Standardization; 2014

[18] S. H. Chen, L.Q. Li, Y. B. Chen. Interfacial reaction mode and its influence on tensile strength in laser joining Al alloy to Ti alloy. Materials Science and Technology, 26 (2010), pp. 230-235.

[19] AWS D17.2/D17.2M. Specification for Resistance Welding for Aerospace Applications. In: American Society Welding; 2013.

[20] T. Rosendo, B. Parra, M.A.D. Tier, A.A.M. da Silva, J.F. dos Santos, T.R. Strohaecker, N.G. Alcântara. Mechanical and microstructural investigation of friction spot welded AA6181-T4 aluminium alloy. Materials & Design, 32 (2011), pp. 1094-1100.

[21] T. Tanaka, T. Morishige, T. Hirata. Comprehensive analysis of joint strength for dissimilar friction stir welds of mild steel to aluminum alloys. Scripta Materialia 61 (2009), pp. 756–759.

[22] A. Wu, Z. Song, K. Nakata, J. Liao, L. Zhou. Interface and properties of the friction stir welded joints of titanium alloy Ti6Al4V with aluminum alloy 6061. Materials & Design 71 (2015), pp. 85-92.

[23] J.R.W.D. Callister Materials science and engineering: an introduction (7th ed.) John Wiley & Sons (2007).

[24] U. Suhuddin, V. Fischer, F. Kroeff, J.F. dos Santos. Microstructure and mechanical properties of friction spot welds of dissimilar AA5754 Al and AZ31 Mg alloys. Materials Science and Engineering: A, 590 (2014), pp. 384-389.